Association of Heat Production with ^{18}F-FDG Accumulation in Murine Brown Adipose Tissue After Stress

Edward A. Carter[1–3], Ali A. Bonab[2–4], Kasie Paul[2], John Yerxa[2,5], Ronald G. Tompkins[2,3,5], and Alan J. Fischman[3]

[1]Department of Pediatrics, Massachusetts General Hospital, Boston, Massachusetts; [2]Harvard Medical School, Boston, Massachusetts; [3]Shriners Hospitals for Children, Boston, Massachusetts; [4]Nuclear Medicine and Molecular Imaging, Massachusetts General Hospital, Boston, Massachusetts; and [5]Department of Surgery, Massachusetts General Hospital, Boston, Massachusetts

Previous studies have demonstrated that cold stress results in increased accumulation of ^{18}F-FDG in brown adipose tissue (BAT). Although it has been assumed that this effect is associated with increased thermogenesis by BAT, direct measurements of this phenomenon have not been reported. In the current investigation, we evaluated the relationship between stimulation of ^{18}F-FDG accumulation in BAT by 3 stressors and heat production measured in vivo by thermal imaging. Male SKH-1 hairless mice were subjected to full-thickness thermal injury (30% of total body surface area), cold stress (4°C for 24 h), or cutaneous wounds. Groups of 6 animals with each treatment were kept fasting overnight and injected with ^{18}F-FDG. Sixty minutes after injection, the mice were sacrificed, and biodistribution was measured. Other groups of 6 animals subjected to the 3 stressors were studied by thermal imaging, and the difference in temperature between BAT and adjacent tissue was recorded (ΔT). Additional groups of 6 animals were studied by both thermal imaging and ^{18}F-FDG biodistribution in the same animals. Accumulation of ^{18}F-FDG in BAT was significantly ($P < 0.0001$) increased by all 3 treatments (burn, ~5-fold; cold, ~15-fold; and cutaneous wound, ~15-fold), whereas accumulation by adjacent white adipose tissue was unchanged. Compared with sham control mice, in animals exposed to all 3 stressors, ΔTs showed significant ($P < 0.001$) increases. The ΔT between stressor groups was not significant; however, there was a highly significant linear correlation ($r^2 = 0.835$, $P < 0.0001$) between the ΔT measured in BAT versus adjacent tissue and ^{18}F-FDG accumulation. These results establish, for the first time to our knowledge, that changes in BAT temperature determined in vivo by thermal imaging parallel increases in ^{18}F-FDG accumulation.

Key Words: animal imaging; molecular imaging; PET

J Nucl Med 2011; 52:1616–1620
DOI: 10.2967/jnumed.111.090175

Brown adipose tissue (BAT) and white adipose tissue (WAT) are both present in mammals. The primary function of WAT is lipid storage, whereas BAT is intimately involved in energy metabolism. BAT is especially abundant in newborns and hibernating mammals (*1*), in whom its primary function is to generate body heat by nonshivering thermogenesis. The mechanism for this process is believed to be related to uncoupling of substrate use and adenosine triphosphate production in mitochondria, with resulting dissipation of metabolic energy as heat (*2*).

Until recently, the interpretations of ^{18}F-FDG PET studies were confounded by the presence of focal areas of increased tracer accumulation in the supraclavicular region, intercostal region, periadrenal region, and axilla and around the great vessels—a finding that was erroneously ascribed to nodal disease. With the introduction of PET/CT, this finding was confirmed to represent focal areas of BAT. Accumulation of ^{18}F-FDG in BAT has been shown to be particularly prominent in lean females during the cold months (*3–7*).

Cold stress has also been shown to activate ^{18}F-FDG accumulation in BAT in rodents (*8*). In addition, BAT has been considered to be important in insulin resistance—a condition in which insulin is unable to lower glucose levels (*9*). In previous reports, we studied the effects of cold stress, burn injury, and cutaneous wounds on BAT at the macroscopic, microscopic, and metabolic levels (*10–12*) in mice. The findings of these studies indicated that all 3 stressors significantly affect BAT at the structural and functional levels. In a subsequent study, we demonstrated that there is a temporal and size relationship between the stressors and stimulation of ^{18}F-FDG accumulation in BAT (*13*). In the present investigation, we examined whether the stimulation of ^{18}F-FDG accumulation in BAT is associated with increased heat production in vivo by thermal imaging.

Although it has been assumed that increased ^{18}F-FDG accumulation in BAT is associated with increased thermogenesis, direct measurements of this phenomenon have not been reported. The findings of the current study establish, for the first time to our knowledge, that changes in BAT temperature determined in vivo by thermal imaging parallel increases in ^{18}F-FDG accumulation.

Received Mar. 8, 2011; revision accepted Jun. 22, 2011.
For correspondence or reprints contact: Edward A. Carter, Massachusetts General Hospital, Fruit St., Boston, MA 02114.
E-mail: carter.ea@gmail.com
Published online Sep. 13, 2011.

MATERIALS AND METHODS

Materials

^{18}F-labeled FDG prepared by routine methods (*14*) was purchased from PetNet.

Animal Preparation

Male CD-1 or SKH-1 hairless mice (28–30 g, Charles River) were used in these studies. After delivery, the animals were acclimatized to the animal facility of Massachusetts General Hospital for at least 5 d in a room in which the temperature was maintained at 20°C ± 1°C with a 12 h–12 h light–dark cycle. After acclimatization, the animals were treated as described in the following sections. A time line for the basic procedures is shown in Figure 1.

Effect of Shaving

CD-1 mice were anesthetized with ether, and their dorsum was shaven. The mice were allowed to recover for 24 h in mesh-bottom cages without food but with water ab libitum before thermal imaging.

Burn Injury

Full-thickness, nonlethal thermal injury was produced as described previously (*15*). Briefly, under ether anesthesia, the mice were placed in molds exposing 30% of total body surface area on the lower dorsum to water at 90°C for 9 s. The animals were immediately resuscitated with saline (15 mL/kg) by intraperitoneal injection. Sham control animals were treated similarly, with the exception that the water was at room temperature. After the procedure, the animals were caged individually in mesh-bottom cages, and water was provided ab libitum. The mice were kept fasting overnight at room temperature before radiopharmaceutical administration.

Cold Stress

To produce cold stress, the mice were placed in a cold room at 4°C for 24 h with overnight fasting with water provided ab libitum. The mice were housed 3 to a cage in mesh-bottom cages, and the radiopharmaceutical was administered on the following morning.

Cutaneous Wounds

For the cutaneous wound procedure, the mice were anesthetized and a 1 cm^2 section of skin was removed to the level of the fascia to produce a full-thickness wound. After the procedure, the mice were housed individually in wire mesh-bottom cages and kept fasting overnight at room temperature, with water provided ab libitum before radiopharmaceutical administration.

Animal Care Approval

Animal care was provided in accordance with the procedures outlined by the *Guide for the Care and Use of Laboratory Animals* (*16*). The study was approved by the Subcommittee on Research Animal Care of the Massachusetts General Hospital. All animals survived the procedures, consumed water, and moved freely in their cages without apparent distress

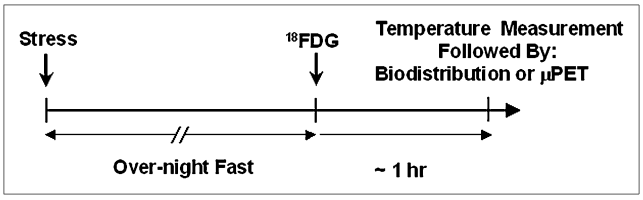

FIGURE 1. Time line for studies. Stress indicates cold stress, burn injury, or cutaneous wound. Temperature measurements by thermal imaging were performed at 55 min after ^{18}F-FDG injection and were followed by biodistribution measurements or small-animal PET. Six animals were studied with each treatment. μPET = small-animal PET.

Biodistribution Studies

The fasted animals were injected (without anesthesia) via the tail vein with ^{18}F-FDG (1.85 MBq [50.0 μCi]). One hour after tracer administration, the animals were sacrificed; selected tissues were excised and weighed; and biodistribution was measured. Tissue radioactivity was measured with a Wizard γ-counter (Wallac). Radioactivity in aliquots of the injected doses was measured in parallel with the tissue samples to correct for radioactive decay. All results were expressed as percentage injected dose per gram of tissue (%ID/g; mean ± SEM).

Thermal Imaging

Mice (unanesthetized or anesthetized) were imaged with a thermal imaging camera (CTI-TIP; sensitivity 0.001°C). The pixel size was 0.3 × 0.3 mm. The mice were placed on a metal grid in a plastic box 30 cm below the camera. The tail of each mouse was held gently, to partially immobilize the animal for the 5 s needed to record the temperature of the dorsum. The temperature of the BAT and adjacent tissue was determined by placing the cursor on the area to be tested and manually recording the temperature displayed by the computer. Because the temperature was quite uniform over the interscapular region and the color scale represents 1°C increments in temperature, the BAT temperature was assigned to the value at the central pixel. The outer boundary of the region was defined as an area with 1°C lower temperature. The areas tested were confirmed as BAT or WAT at necropsy. The difference in temperature between BAT and adjacent tissue was recorded (ΔT). The results were expressed as ΔT (mean ± SEM).

Thermal Imaging and ^{18}F-FDG Biodistribution in Same Animals

Thermal imaging and ^{18}F-FDG biodistribution studies were performed in additional groups of 6 animals exposed to the same stressors. For these studies, the mice were injected with ^{18}F-FDG, and ΔT was determined immediately before sacrifice and measurement of biodistribution. Percentage of dose injected per gram of wet tissue of ^{18}F-FDG versus %ΔT was plotted for each animal, and linear regression analysis was performed.

Small-Animal PET Studies

To further evaluate glucose metabolism in major organs, ^{18}F-FDG small-animal PET was conducted for a subset of the animals. Imaging was performed with a Concord P4 small-animal PET device. One hour after intravenous injection of ^{18}F-FDG (~0.0185 MBq [~0.5 μCi]), the mice were anesthetized and stabilized in the gantry of the camera, and a 10-min image was acquired in list mode. The primary imaging characteristics of the P4 camera are an average intrinsic spatial resolution of approximately 2 mm in full width at half maximum, 63 contiguous slices of 1.21-mm separation, and a sensitivity of approximately 650 cps/μCi. A small water cylinder with known amount of ^{18}F-FDG was used to calibrate the camera to nCi/mL. This calibration factor was in the normalization files that was used to reconstruct the images. The data were reconstructed using an iterative algorithm, maximum a posteriori, in a 256 × 256 matrix with a zoom of 4. Data for attenuation correction were measured with a rotating point source containing ^{57}Co. All projection data were corrected for non-

uniformity of detector response, dead time, random coincidences, and scattered radiation. The PET camera was cross-calibrated to a well scintillation counter by comparing the camera response from a uniform distribution of an ^{18}F solution in a 5.0-cm-diameter cylindric phantom with the response of the well counter to an aliquot of the same solution.

Statistical Analysis

Statistical analysis was performed by 1-way ANOVA or linear regression. Individual means were compared by Duncan multiple-range testing. Results with P values of less than 0.05 were considered to be statistically significant.

RESULTS

Thermal Imaging of SKH-1 Mice

Figure 2 illustrates typical thermal images of an unanesthetized hairless mouse with burn injury and a sham-treated control. Higher temperatures are in the purple range, and lower temperatures are in green. Mice with burn injury consistently exhibited an area on the upper dorsum with higher ΔT than sham controls. The area with the highest recorded ΔT was in the interscapular region, in which BAT is most prominent, as confirmed by surgical examination. The area adjacent to the BAT showed a lower temperature and was surgically confirmed to be WAT.

Thermal images of shaven CD-1 mice demonstrated diffusely increased ΔT in the dorsum (data not shown), most probably due to irritation produced by shaving. Thus, SKH-1 mice were used in the comparative stressor studies.

Effect of Stressors on ^{18}F-FDG Accumulation in BAT in SKH-1 Hairless Mice

As can be seen in Figure 3, application of cold stress, burn injury, and cutaneous wound 24 h previously resulted in increased ^{18}F-FDG accumulation in BAT. ANOVA showed a significant main effect of treatment ($F_{3,23} = 149.08$; $P < 0.0001$). All 3 stressors produced significant increases in BAT accumulation of ^{18}F-FDG when compared with sham control animals (cold and cutaneous wound [$P < 0.0001$] and burn injury [$P < 0.001$]). The increases in ^{18}F-FDG associated with cold and cutaneous wounds were significantly greater than the increase associated with burn injury ($P < 0.0001$). Overall, cold and cutaneous wounds produced approximately 15-fold increases in ^{18}F-FDG, compared with sham control animals, whereas burn injury produced an approximately 5-fold increase.

Small-Animal PET Studies

Representative ^{18}F-FDG small-animal PET images (sagittal slices) of a sham control hairless mouse and a hairless mouse subjected to cold stress are shown in Figure 4. ^{18}F-FDG small-animal PET demonstrated intense focal uptake at sites of BAT after cold stress. Uptake in BAT was so intense

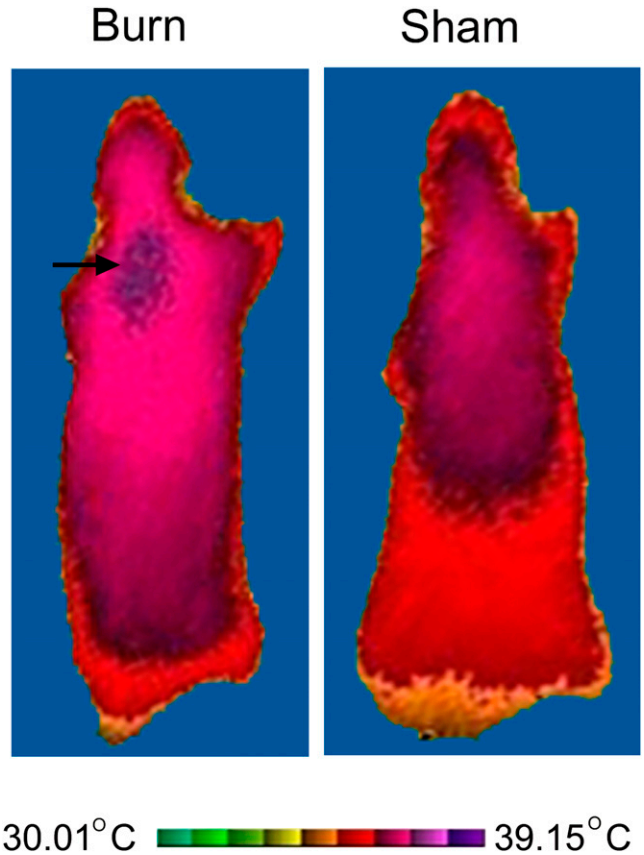

FIGURE 2. Thermal images of sham unanesthetized fasted SKH-1 hairless mouse with burn injury and sham-treated control. Mice were all imaged at same time after injury. Arrow indicates region of interscapular BAT in burned mouse. Temperature scale = ~30°C–39°C (green-purple).

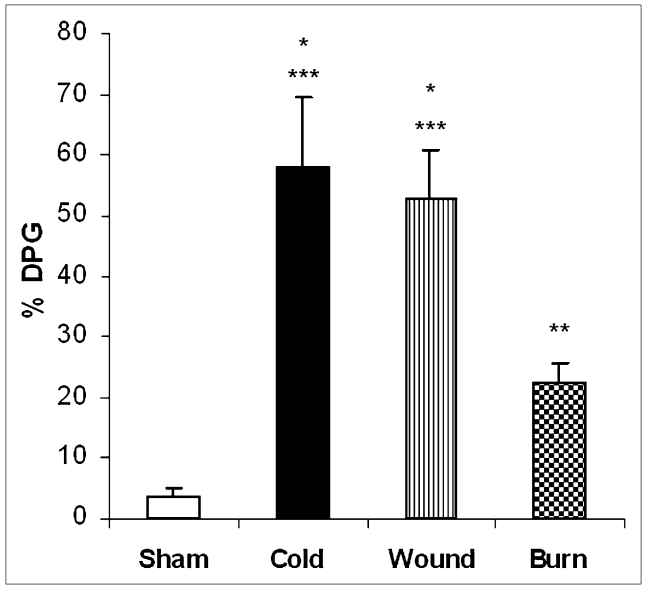

FIGURE 3. Effect of cold stress, cutaneous wound, and burn injury on ^{18}F-FDG accumulation in BAT in hairless mice. Mice were treated as described in "Materials and Methods" section. There were 6 mice in each group. Values are expressed as %ID/g, mean ± SEM. $^{*}P < 0.0001$ vs. sham treated control mice. $^{**}P < 0.001$ vs. sham-treated control mice. $^{***}P < 0.0001$ vs. mice with burn injury. %DPG = percentage of dose injected per gram of wet tissue.

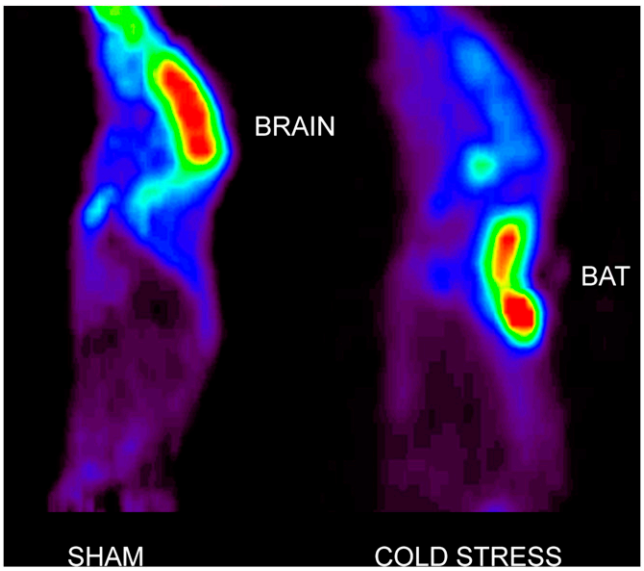

FIGURE 4. Representative ^{18}F-FDG-small-animal PET images of sham-treated and cold-stressed mice. Uptake in BAT was so intense that it was associated with significant reductions in uptake by all other tissues, including brain.

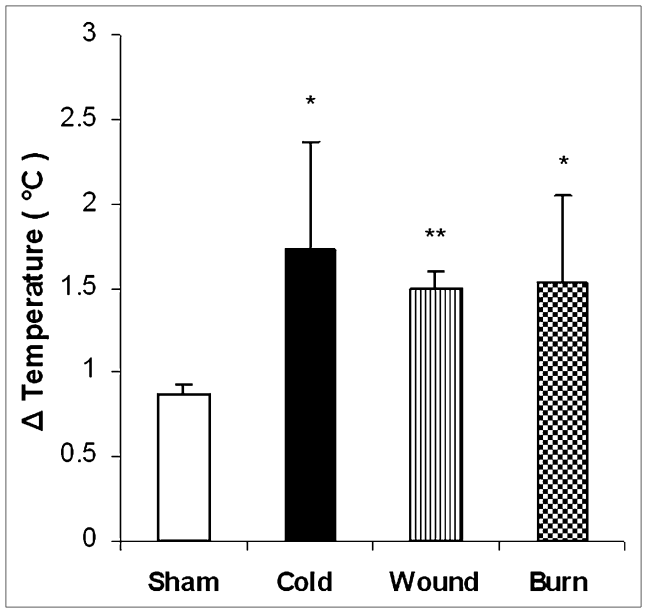

FIGURE 5. Effect of cold stress, cutaneous wound, and burn injury on ΔT of BAT. Mice were treated as described in "Materials and Methods" section. There were 6 mice in each group. Values are expressed as difference in temperature between BAT and adjacent area (ΔT, mean ± SEM). *$P < 0.01$ vs. sham treated control mice. **$P < 0.001$ vs. sham-treated control mice.

that it was associated with significant reductions in uptake by all other tissues, including the brain.

Thermal Imaging of Effect of Stressors on Heat Production by BAT In Vivo

As illustrated in Figure 5, the application of cold stress, burn injury, and cutaneous wound 24 h previously resulted in increased BAT temperature. ANOVA showed a significant main effect of treatment ($F_{3,23} = 8.71$; $P < 0.001$). All 3 stressors produced significant increases in the temperature of BAT when compared with sham control animals (cutaneous wound [$P < 0.0001$] and cold and burn injury [$P < 0.01$]). However, the effects of the treatments were not significantly different. As illustrated in Figure 6, regression analysis demonstrated a highly significant linear relationship between ^{18}F-FDG accumulation in BAT determined by biodistribution measurements and ΔT determined by thermal imaging ($r^2 = 0.835$, $P < 0.0001$).

DISCUSSION

Although nonshivering thermogenesis is usually considered to be important in hibernating animals and to some extent in children, recent ^{18}F-FDG PET studies have demonstrated significant BAT activity in adults, particularly during cold months (*3,4,6–8*). In this report, we studied the relationship between ^{18}F-FDG accumulation in BAT determined by biodistribution and the associated temperature changes in BAT, compared with adjacent tissue, as determined in vivo by thermal imaging.

In the present study, we used SKH-1 hairless mice to determine whether the 3 stressors affected BAT temperature, compared with adjacent tissues, in vivo by thermal imaging. The use of hairless mice in skin research has been reviewed recently (*17*). We chose to use the hairless mouse for our studies because it eliminates variability in the removal of hair over the BAT area. Mice with hair could have been treated with a chemical hair remover after shaving to produce a hairless mouse. However, we have found that this treatment increases mortality after burn injury because histologic examination of tissue from these animals shows signs of injury (Ed Carter, unpublished data, 2010). Studies using thermal imaging cameras rely on measurement of the temperature of the area in question and a reference point, yielding a change in temperature between the 2 areas. For our studies, we used the point at which BAT is expected to be present in large amounts (interscapular region) and the adjacent area.

We first confirmed that ^{18}F-FDG accumulation in BAT was activated by cold, burn injury, or cutaneous wound. We then used thermal imaging to noninvasively measure brown fat temperature, compared with adjacent tissue. Finally we determined whether there was a relationship between the change in BAT temperature, compared with adjacent tissue, and ^{18}F-FDG accumulation in BAT after activation by cold, burn injury, or cutaneous wound.

One of the primary functions of BAT is to produce heat (*18*). The law of constant heat summation formulated by Hess states that the decrease in enthalpy of a reaction sequence (the heat that evolves at constant pressure) depends only on the initial reactants and final products of the sequence and is independent of the intervening reaction steps. Consequently, the heat that evolves by the oxidation of a substrate such as glucose in BAT will be the same when a direct chemical combustion occurs as when a

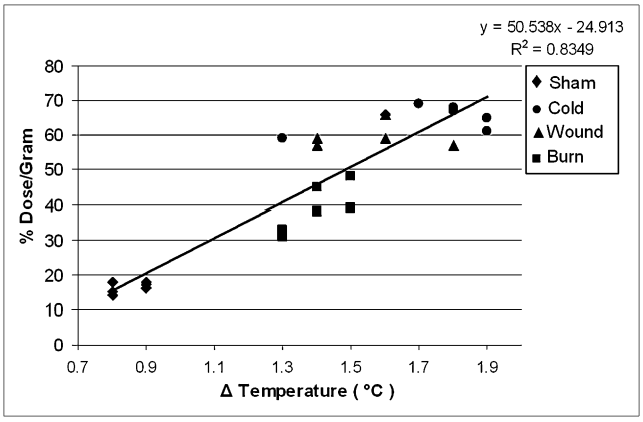

FIGURE 6. Linear regression analysis of temperature and ^{18}F-FDG accumulation in BAT of hairless mice. Mice were treated as described in "Materials and Methods" section. Values are expressed as difference in temperature between BAT and adjacent area vs. percentage ^{18}F-FDG accumulation per gram of tissue. There was significant linear correlation ($r^2 = 0.835$, $P < 0.0001$) between ΔT measured in BAT vs. adjacent tissue in vivo and ^{18}F-FDG accumulation determined by biodistribution measurements.

brown adipocyte catalyzes the same overall reaction through a cascade of some 30 enzymatic steps (*18*).

Nagashima et al. (*19*) and Inokuma et al. (*20*) have demonstrated increased heat production by BAT under the influence of norepinephrine. These studies involved insertion of a temperature probe directly into the BAT. The disadvantage of this approach is that the animal must be anesthetized and it has been demonstrated that anesthesia, especially with volatile anesthetics, can alter BAT function (*21*). In addition, there will be some surgical manipulation of the area. Furthermore, insertion of the temperature probe may introduce a sampling error unless the area is surgically manipulated to document the exact location of BAT versus WAT. An alternative approach would be to insert devices to monitor BAT temperature continuously. However, this procedure also requires surgical manipulations that could introduce sampling errors.

CONCLUSION

Our results indicate that activation of ^{18}F-FDG accumulation in BAT after cold stress, burn injury, and cutaneous wound is correlated with an increase in BAT temperature, compared with adjacent tissue as measured by thermal imaging. Clearly, thermal imaging of hairless mice represents an attractive experimental model for screening drugs for their effects on BAT activation as treatments for conditions such as diabetes mellitus.

DISCLOSURE STATEMENT

The costs of publication of this article were defrayed in part by the payment of page charges. Therefore, and solely to indicate this fact, this article is hereby marked "advertisement" in accordance with 18 USC section 1734.

ACKNOWLEDGMENTS

This study was supported in part by grants from the National Institutes of Health (2P50 GM 021700-27A) and Shriners Hospitals for Children (grant 8470). No other potential conflict of interest relevant to this article was reported.

REFERENCES

1. Cannon B, Nedergaard J. Brown adipose tissue: function and physiological significance. *Physiol Rev.* 2004;84:277–359.
2. Sell H, Deshaies Y, Richard D. The brown adipocyte: update on its metabolic role. *Int J Biochem Cell Biol.* 2004;36:2098–2104.
3. van Marken Lichtenbelt WD, Vanhommerig JW, Smulders NM, et al. Cold-activated brown adipose tissue in healthy men. *N Engl J Med.* 2009;360:1500–1508.
4. Cypess AM, Lehman S, Williams G, et al. Identification and importance of brown adipose tissue in adult humans. *N Engl J Med.* 2009;360:1509–1517.
5. Virtanen KA, Lidell ME, Orava J, et al. Functional brown adipose tissue in healthy adults. *N Engl J Med.* 2009;360:1518–1525.
6. Saito M, Okamatsu-Ogura Y, Matsushita M, et al. High incidence of metabolically active brown adipose tissue in healthy adult humans: effects of cold exposure and adiposity. *Diabetes.* 2009;58:1526–1531.
7. Au-Yong IT, Thorn N, Ganatra R, Perkins AC, Symonds ME. Brown adipose tissue and seasonal variation in humans. *Diabetes.* 2009;58:2583–2587.
8. Tatsumi M, Engles JM, Ishimori T, Nicely O, Cohade C, Wahl RL. Intense ^{18}F-FDG uptake in brown fat can be reduced pharmacologically. *J Nucl Med.* 2004;45:1189–1193.
9. Valverde AM, Benito M. The brown adipose cell: a unique model for understanding the molecular mechanism of insulin resistance. *Mini Rev Med Chem.* 2005;5:269–278.
10. Carter EA, Ma BY, Mcintosh LJ, Cyr E, Fischman AJ, Tompkins RG. Burn injury or cutaneous wound injury to mice stimulates brown fat but not white fat uptake of F18-FDG in vivo. *J Burn Care Res.* 2006;27:S166.
11. Carter E, McIntosh L, Cyr E, et al. Cold-stress, dermal wound and burn injury stimulate uptake of FDG by brown adipose tissue (BAT) in mice: relationship with uncoupling protein 1 expression [abstract]. *J Nucl Med.* 2006; 47:343P.
12. Carter EA, Bonab AA, Hamrahi V, et al. Effects of burn injury, cold stress and cutaneous wound injury on the morphology and energy metabolism of murine brown adipose tissue (BAT) in vivo. *Life Sci.* 2011;89:78–85.
13. Cater EA, Winter D, Dagostino P, Tompkins RG, Fischman AJ. Burn injury stimulation of FDG uptake by brown adipose tissue (BAT): effects of lesion position, extent and time after injury [abstract]. *J Nucl Med.* 2007;48:270P.
14. Hamacher K, Coenen HH, Stocklin G. Efficient stereospecific synthesis of no-carrier-added 2-[^{18}F]-fluoro- 2-deoxy-D-glucose using aminopolyether supported nucleophilic substitution. *J Nucl Med.* 1986;27:235–238.
15. Zhang Q, Carter EA, Ma BY, White M, Fischman AJ, Tompkins RG. Molecular mechanism(s) of burn-induced insulin resistance in murine skeletal muscle: role of IRS phosphorylation. *Life Sci.* 2005;77:3068–3077.
16. *Guide for the Care and Use of Laboratory Animals*. Washington, DC: National Academy Press; 1996.
17. Benavides F, Oberyszyn TM, VanBuskirk AM, Reeve VE, Kusewitt DF. The hairless mouse in skin research. *J Dermatol Sci.* 2009;53:10–18.
18. Nichols DG, Locke RM. Thermogenic mechanisms in brown fat. *Physiol Rev.* 1984;64:1–64.
19. Nagashima T, Ohinata H, Kuroshima A. Involvement of nitric oxide in noradrenaline-induced increase in blood flow through brown adipose tissue. *Life Sci.* 1994;54:17–25.
20. Inokuma K, Ogura-Okamatsu Y, Toda C, Kimura K, Yamashita H, Saito M. Uncoupling protein 1 is not necessary for norepinephrin-induced glucose utilization in brown adipose tissue. *Diabetes.* 2005;54:1385–1391.
21. Ohlson KBE, Lindahl SGE, Cannon B, Nedergaard J. Thermogenesis inhibition in brown adipocytes is a specific property of volatile anesthetics. *Anesthesiology.* 2003;98:437–448.

The Journal of NUCLEAR MEDICINE

Association of Heat Production with ^{18}F-FDG Accumulation in Murine Brown Adipose Tissue After Stress

Edward A. Carter, Ali A. Bonab, Kasie Paul, John Yerxa, Ronald G. Tompkins and Alan J. Fischman

J Nucl Med. 2011;52:1616-1620.
Published online: September 13, 2011.
Doi: 10.2967/jnumed.111.090175

The Journal of Nuclear Medicine is published monthly.
SNMMI | Society of Nuclear Medicine and Molecular Imaging
1850 Samuel Morse Drive, Reston, VA 20190.
(Print ISSN: 0161-5505, Online ISSN: 2159-662X)

SNMMI SOCIETY OF NUCLEAR MEDICINE AND MOLECULAR IMAGING